Tetracycline Removal Enhancement With Fe-Saturated Nanoporous Montmorillonite in a Tripartite Adsorption/Desorption/Photo-Fenton Degradation Process

Shiva Chahardahmasoumi
Isfahan University of Technology
Seyed Amir Hossein Jalali
Isfahan University of Technology
Mehdi Nasiri Sarvi (mnsarvi@iut.ac.ir)
Isfahan University of Technology https://orcid.org/0000-0002-8172-2077

Research Article

Keywords: Montmorillonite, Photo-Fenton, Nanoporous, Tetracycline, Adsorption, Desorption, Fe-saturated

Posted Date: October 29th, 2021

DOI: https://doi.org/10.21203/rs.3.rs-1000024/v1

Abstract

The adsorption and photo-Fenton degradation of tetracycline (TC) over Fe saturated nanoporous montmorillonite was analyzed. The synthesized samples were characterized using XRD, FTIR, SEM, and XRF analysis, and the adsorption and desorption of TC onto these samples as well as the antimicrobial activity of TC during these processes were analyzed at different pH. The results indicated that the montmorillonite is a great adsorbent for the separation of the TC from aqueous solutions, however, after increasing the amount of TC adsorbed, the desorption process started, and up to 50% of TC adsorbed onto non-modified montmorillonite was released back to the solution with almost no changes in its antimicrobial activity. After acid treatment (for creation of nanoporous layers) and Fe saturation of the montmorillonite, almost similar great separation was achieved compared to non-modified montmorillonite. In addition, the desorption of TC from modified montmorillonite was still high up to 40% of adsorbed TC. However, simultaneous adsorption and photodegradation of TC were detected and almost no antimicrobial activity was detected after 180 min of visible light irradiation, which could be due to the photo-Fenton degradation of TC on the modified montmorillonite surface. In the porous structures of modified montmorillonite high $^{\cdot}OH$ radicals were created in the photo-Fenton reaction and were measured using the Coumarin technique. The $^{\cdot}OH$ radicals help the degradation of TC as proposed in an oxidation process. Surprisingly, more than 90 % of antimicrobial activity of the TC decreased under visible light (after 180 min) when desorbed from nanoporous Fe-saturated montmorillonite compared to natural montmorillonite. To the best of our knowledge, this is the first time that such a high TC desorption rate from an adsorbent with the least remained antimicrobial activity is reported which makes nanoporous Fe-saturated montmorillonite a perfect separation substance of TC from the environment.

1. Introduction

The release of active metabolite species of antibiotics in the ecosystem cycle and the prevalence of a new generation of antibiotic-resistant bacteria and genes have caused a global concern over their threats to mankind (Imanipoor et al. 2021, Liu et al. 2021a, Mosaleheh &Sarvi 2020, Wang et al. 2020a, Wu et al. 2018). Tetracycline (TC) is recognized as the second most widely consumed antibiotic, which is extensively distributed in the environment due to its high-water solubility and low absorption rate by men, livestock, and poultry (*i.e.* about 10 to 40%) (Jiao et al. 2008, Norvill et al. 2017, Shen et al. 2020, Zhang et al. 2017). TC was considered as a potential agent able to change and evolve genetic features of bacteria and thereby resulting in the emergence of a new generation of antibiotic-resistant bacteria (Ramazani Afarani et al. 2018, Verma &Haritash 2020). The successful application of TC for recently emmerged viruses, might resulted in an unexpected increase of TC in the environment. Recent studies suggested that the early use of TC prevent viral infection to serious infection in COVID-19 (Mosquera-Sulbaran &Hernández-Fonseca 2021). Besides, as the promissing results of TC in treatment of COVID-19 patients with mild symptoms (Gironi et al. 2021), it seams that the use of this antibiotics is increasing and consequently new strategies have to be developed for its removal from the environment.

Different techniques have been developed for separation of antibiotics from the environment such as adsorption and catalysis degradation (Jain et al. 2020, Niu et al. 2021). Adsorption, as one of the most effective separation techniques, has been developed by many scientists, and numerous adsorption substances have been synthesized and modified for this purpose (Ahsan et al. 2018, Wang et al. 2021, Zhao et al. 2015). When looking at the adsorption technique as a practical method, the development of environmentally friendly adsorbents with the least residual environmental side effects, low secondary environmental pollution, high adsorption efficiency, and low-cost production become crucial (Mosaleheh &Sarvi 2020, Veiskarami et al. 2016). Besides, due to the abundance of antibiotics and possible residual antimicrobial activity of adsorbed antibiotics, providing a low release tendency or employing a degradation capability on the adsorbent to reduce the chance of secondary pollution has been the goal of many researchers (Bugueño-Carrasco et al. 2021, Lu et al. 2019a, Lu et al. 2019b).

The degradation of bio-contaminants with a photocatalytic process has recently been converted to a promising method having high efficiency, high degradation rate, and the least side effects (Hassan et al. 2019, Huang et al. 2020, Li et al. 2021). Photocatalyst substance accelerates the decomposition of biomolecules through the production of reactive species (Thomas et al. 2021). Hence the development of photocatalysts with the features mentioned above has become a controversial topic related to environmental problems. Hence, the development of a combined adsorption and photodegradation process could help to increase the efficiency of the separation method practically. Photo-Fenton process is a promising process for the degradation of antibiotics, such as TC (Han et al. 2020, Tong et al. 2021, V. M. Starling et al. 2021, Wang et al. 2020b). This process, as an advanced oxidation process, is widely used for the treatment of antibiotics contaminated media (Ameta et al. 2018). This is one of the most environmentally friendly processes with the least secondary pollution and residual side effects (Wang et al. 2020b).

Montmorillonite has been used for the adsorption of different biomolecules (Akbari Alavijeh et al. 2017, Ambrogi et al. 2014, Imanipoor et al. 2021, Jayrajsinh et al. 2017). Moreover, it has such an extent potential to use as a barrier for halting the spread of pollutants in the environments due to its high cation exchange and adsorption capacity, eco-friendly nature, and non-toxicity (Carretero et al. 2013, Zhao et al. 2015). Nevertheless, modifying the montmorillonite layered structure into a photocatalyst was proposed to decompose the adsorbed bio-components (Chen et al. 2009). Although montmorillonite was reported to have great adsorption characteristics, the release of the adsorbed antibiotics after saturation of the layered structure (Akbari Alavijeh et al. 2017, Ramazani Afarani et al. 2018) reduces the chance of using that for adsorption. In addition, its layered structure which prevents the penetration of light beams in the structures (Ambrogi et al. 2012) reduces its efficiency when used as a photocatalyst. These problems limit the application of montmorillonite and photocatalyst-loaded montmorillonite as a potential separation media for different antibiotics (Maroga Mboula et al. 2012).

In this research, montmorillonite was modified to improve its mutual function for adsorption and photodegradation of the tetracycline. For this purpose, an acid treatment was applied to create nanopores onto its layered structure with more active sites for the adsorption as well as photoreaction. Besides, the

layered structure of the montmorillonite was saturated with the Fe ions to improve the photo-Fenton degradation process of the adsorbed TC. In the separation process, the adsorption and desorption of TC from montmorillonite were characterized and the photodegradation after the adsorption/desorption cycle was analyzed.

2. Materials And Methods

2.1. Materials

Bentonite as a source of montmorillonite was purchased from a bentonite mine located in Salafchegan, Iran with a CEC of 73 mEq/100gr. Tetracycline hydrochloride (> 98%, Sigma Aldrich), hydrochloric acid (HCl, 37% w/w, Merck), and hydrogen peroxide (H_2O_2, 30% w/w, Merck) were used as received. Coumarin was provided by Sigma Aldrich and used as received. Deionized water was used for all experiments. A visible halogen light lamp was used as the light source for photocatalyst experiments.

2.2. Montmorillonite modification

The particles of montmorillonite smaller than 2.5 microns were separated using centrifuge force (Veiskarami et al. 2016). Typically, a 3% (w/v) solution of bentonite in water was prepared and mixed overnight at 25 ºC. Afterward, the obtained suspension was centrifuged at 1000 rpm, 25 ºC for 260 s. The supernatant was collected and dried at 60 ºC overnight and named Mt. To prepare a nanoporous montmorillonite sample the Mt sample was then reacted with 1 M HCl at boiling temperature for 60 minutes. After completing the acid treatment, the mixture was centrifuged at 5000 rpm, 25ºC for 5 minutes. The precipitates were washed with plenty of water several times, dried at 60 ºC overnight, and named NP-Mt.

The two montmorillonite samples (Mt and NP-Mt) were then saturated with Fe^{+3} (Hong et al. 2019). For this purpose, the montmorillonite samples were added to a 0.1 M $FeCl_3$ solution for two hours, and this process was repeated several times. An excess amount of iron was washed with water and then the samples were then separated using centrifuge force and dried in an oven at 60 ºC overnight. All samples were kept in a desiccator containing silica gel before use.

2.3. Kinetic of adsorption and desorption of TC

The kinetic adsorption experiments were carried out in 12 intervals of 1, 2, 4, 8, 15, 30, 60, 90, 120, 180, 240, and 400 minutes at 25 ºC and a dark condition. Typically, 100 mg of montmorillonite sample was mixed with 20 ml of TC solution (1 mg/ml) at three different pH of 5, 7, and 9. Afterward, the mixture was centrifuged at 5000 rpm, 25 ºC for 7 minutes, and the TC concentration of the supernatant was measured using a UV-Visible spectrophotometer at wavelength 276 nm. Finally, the amount of adsorbed TC was calculated based on the mass balance, according to a prepared standard curve.

Desorption kinetic experiments were designed to investigate the amount of TC desorption after adsorption on montmorillonite samples. Typically, after 8 hours of mixing of montmorillonite with TC

solution (according to kinetic adsorption results), the solution was centrifuged and the precipitates (montmorillonite-TC hybrid) were added to a rotating 500 ml balloon which contained a 250 ml of the receptor solution (with the same pH of adsorption) and covered with aluminum foil (the temperature was set at 25 ºC using a water bath). The amount of desorbed TC was monitored via measuring the concentration of the balloon solution at different intervals (9, 18, 27, 36, 45, 54, 63, 72, 81, 90, 99, 108, 117, 126, 150, 174, 198, and 225 minutes) using a UV-Visible spectrophotometer at wavelength of 276 nm. The balloon was charged with the exact amount of samples that were taken with the fresh receptor.

2.4. Tetracycline photo-Fenton degradation

The photo-induced changes in TC by the montmorillonite samples were then studied. Generally, all the experiments were performed using a halogen light lamp, which was located at a 20 cm distance from samples in a quartz container, and the temperature was set at 25 ºC using a refrigerated incubator. For the photo-Fenton reaction, hydrogen peroxide was added to the mixture before the light irradiation. For each montmorillonite sample, simultaneously two similar series of adsorption tests, as aforementioned, were conducted. Typically, 20 ml of 1 mg/ml TC solution was added to 100 mg of montmorillonite sample, and the mixture was blended at 25 ºC for 8 hours (according to adsorption kinetic results) in a dark condition to reach the maximum adsorption. The mixture was then centrifuged and the precipitates were converted to a quartz container containing 250 ml of black solution with the same pH of adsorption test. One set of samples were then exposed to irradiation under visible light for three durations of 60, 120, and 180 minutes while shaking and the other set of sample were converted to the same solution and shaked in dark. Finally, the antimicrobial activity of the solution was tested for all samples.

2.5. Antibacterial test

The antibacterial activity of TC was evaluated using the agar-disk diffusion method. Muller Hinton agar plates were inoculated with $1.5 * 10^{-8}$ CFU/mL inoculum of *Escherichia coli*. Then, filter paper discs, containing the 300 µL of the TC solutions, which were filtered by syringe filter (0.22-micron), were placed on the agar surface. The Petri dishes were incubated at 37 ˚c for 24 hours. Finally, the inhibition growth zones were analyzed.

2.6. Characterization

A 150W halogen lamp was used as the light source for the photodegradation experiments. Low angle XRD analysis was done in 2θ ranging from 4 to 10 degrees using Rigaku D/max-1200 with Cu Kα irradiation. Ultraviolet-Visible spectroscopy liquid analysis was performed by the Reylight-1600 UV-Visible spectrophotometer to measure the TC concentration in the solution. Scanning electron microscopy (SEM) analysis was used to characterize the morphology of the montmorillonite after treatment using a Zeiss Sigma model (samples were gold-sputtered before analysis). FTIR analysis was conducted using a tensor27 Bruker Fourier spectrometer. Also, the chemical composition of the solid material was determined by Bruker: S4PIONEER X-ray fluorescence (XRF) spectrometer. The nitrogen sorption analysis was done using a Belsorp-mini II Japan, at 77 ºK (the samples were initially degassed for 5 hours at 150 ºC). The coumarin method was used to evaluate the potential for ˙OH radical production (Czili &Horváth

2008, Louit et al. 2005, Maezono et al. 2011). In a typical analysis, 2 ml of coumarin solution (2 mM) was added to the 200 µl sample solution. To ensure almost complete trapping of the ˙OH radical by coumarin, more coumarin solution was added. The ˙OH radicals react with the coumarin molecules, resulting in a highly luminescent 7-hydroxycoumarin. The cell was turned into a detection spectrophotometer equipped with a fluorescent lamp (7 watts near-UV fluorescent lamp). The fluorescent intensity was measured with a spectrophotometer at a wavelength of 470 nm.

3. Results And Discussion

Figure 1 shows the nitrogen sorption results of different montmorillonite samples. All isotherms correspond to H3 hysteresis adsorption associated with capillary condensation in nanopore structures (Sing 1985). The type H3 is normally corresponding to plate-like particles which cause slit-shaped pores (Maged et al. 2020). After acid treatment of montmorillonite, an increase in the surface area of montmorillonite samples was observed (from 28 up to 92 cm^2/g, Table 1), indicating an increase in the porous structures on the montmorillonite layers. This is due to the destruction of the octahedral structure of the montmorillonite (Bieseki et al. 2013, Franco et al. 2016). Besides, the pores volume increased hugely after acid treatment, indicating the formation of nanopores (Table 1). The Fe saturation hardly affected the nitrogen sorption results of the montmorillonite or the acid-treated one. The Fe is enriched on the surfaces of the montmorillonite, however, it is proposed that the Fe is saturated in the removed octahedral sheets of the nanoporous montmorillonite. After acid treatment, the porosity of the montmorillonite (such as specific surface area and pore volume) was increased. Besides, according to XRF analysis (Table 2), most cations (Ca^{2+} and Na^{+}) were leached out from the structure. In addition, the amount of Mg and Fe was slightly reduced, indicating the effect of acid treatment on the montmorillonite.

Table 1
Results of nitrogen sorption analysis

Sample	BET surface area ($m^2\ g^{-1}$)	Pore size (nm)	Total pore volume ($cm^3\ g^{-1}$)
Mt	28		0.12
Mt-Fe	26		0.11
NP-Mt	92		0.40
NP-Mt-Fe	89		0.46

Table 2
XRF analysis of montmorillonite samples

Sample	Mass (%)								
	SiO_2	Al_2O_3	CaO	Fe_2O_3	K_2O	MgO	TiO_2	Na_2O	LOI
Mt	54.5	16.4	1.9	4.1	0.4	3.7	0.4	0.6	18.0
Mt-Fe	51.2	13.5	1.9	11.1	0.3	3.5	0.4	0.5	17.6
NP-Mt	60.8	13.3	0.2	2.1	0.5	2.1	0.4	0.1	20.5
NP-Mt-Fe	56.7	10.6	0.2	11.8	0.5	2.2	0.2	0.1	17.7

The SEM images of samples confirm the layered morphology of montmorillonite and the acid-treated ones (Figure 2). Cracked aggregates, segmented and flaky pieces, and reduced particle size are some of the noteworthy signs of changes in the montmorillonite structure via acid treatment. On both Mt and NP-Mt samples, no significant changes in the structure of montmorillonite occurred after Fe saturation.

FTIR analysis was performed to investigate the changes made to montmorillonite structure through acid treatment (Figure 3). After acid treatment (to provide nanoporous montmorillonite), the intensity of bands at 835, 875, and 914 cm^{-1} decreased, which are corresponding to the bending vibration of AlMgOH, AlFeOH, and Al_2OH, respectively (Franco et al. 2016). This could be due to the leaching of the cations of octahedral sheets by order of Al, Mg, and Fe. In addition to cation removal, and consequently their hydroxyl groups (3620 cm^{-1}), some changes were detected in the intensity of the bands at 1113, 1035, 792, 610, 522, and 462 cm^{-1} (Figure 3). These decreases showed the acid has influenced tetrahedral and octahedral sheets (Si-O-Si, Al-O-Si), and Si-O bands were decomposed partially (Madejová 2003, Maged et al. 2020). Comparing the spectrum of montmorillonite with Fe saturated samples, a new peak emerged at 700 cm^{-1}, which represents the FeOOH bending vibration. This peak suggested that Fe ions are hydrolyzed into the interlayer spaces of the montmorillonite by pillaring (Yuan et al. 2008).

The kinetics of adsorption and desorption of TC onto different montmorillonite samples were plotted in Figure 4 as well as the results of two kinetic models (pseudo-second-order and intraparticle diffusion models) fitted to the data (details of kinetics models are presented in Table 3). For all samples, the equilibrium of adsorption reached after 60 minutes and the Mt and Mt-Fe samples adsorbed more TC than the nanoporous montmorillonite samples to some extent at all pH which is due to the partial destruction of the nanoporous montmorillonite after acid treatment and lower cation exchanges.

Table 3
Details of kinetics models fitted to the adsorption data

Sample	Adsorption pH	Pseudo second order		Intraparticle diffusion					
		k	R^2	k_1	R_1^2	k_2	R_2^2	k_3	R_3^2
Mt	3	0.0121	1	32.5	0.98	8.4	0.91	0.2	0.98
Mt-Fe		0.0125	1	34.5	0.98	8.4	0.91	0.1	0.97
NP-Mt		0.0137	1	27.9	1	7.8	0.92	0.2	0.99
NP-Mt-Fe		0.0133	1	30.1	1	7.6	0.91	0.2	0.98
Mt	5	0.0115	1	33.3	0.98	12.3	1	0.5	0.98
Mt-Fe		0.0118	1	31.7	0.99	9.1	0.96	0.6	0.97
NP-Mt		0.0134	1	27.8	1	7.9	0.98	0.2	0.95
NP-Mt-Fe		0.0138	1	28.9	1	7.1	0.96	0.3	0.95
Mt	8	0.0113	1	33.6	0.98	12.4	0.97	0.4	1
Mt-Fe		0.0124	1	31.2	0.98	11.2	0.99	0.3	0.97
NP-Mt		0.0171	1	22.6	1	5.8	0.99	0.2	0.99
NP-Mt-Fe		0.0184	1	21.8	1	5.1	0.98	0.3	1

The pseudo-second-order model fitted to all data (Figure 4 and Table 3) indicated a similar trend and the adsorption capacity was reduced by increasing the pH. A higher amount of TC adsorbed at lower pH (5 and slightly at 7) which is due to the higher positive charge of TC at this condition (Figueroa et al. 2004) and resulted in a facile cation exchange mechanism (Akbari Alavijeh et al. 2017, Ramazani Afarani et al. 2018). By increasing the pH to 9 higher negative charges of TC resulted in the lower tendency in the adsorption onto the montmorillonite. In addition, lower interlayer adsorption was detected at this condition.

The intraparticle diffusion model results indicated that the adsorption of TC on the external surfaces of all montmorillonite particles was almost the same at all pH of the solution (Figure 4 and Table 3 the first linear region of the plots). At acidic and neutral pH the intraparticle diffusion was another important mechanism of adsorption for all samples which implies the adsorption of TC in the interlayer spaces which will be discussed in the XRD results as well. However, by increasing the pH of adsorption, the intraparticle diffusion reduced for nanoporous samples (acid treated ones) indicating a lower tendency of TC to be diffused in the interlayer spaces due to the higher negative charges of the TC and lower chance of cation exchange mechanism with montmorillonite interlayer cations (Chahardahmasoumi et al. 2019).

The changes in the layered structure of montmorillonite after treatments and adsorption of TC were analyzed using XRD analysis (Figure 5). After acid treatment the basal spacing of the montmorillonite

was increased from 11.6 to 13 Å which could be due to the destruction of the octahedral structure of the montmorillonite upon acid treatment (Temuujin et al. 2004). The saturation of both montmorillonite and nanoporous montmorillonite samples with Fe ion did not affect the basal spacing very much which is in accordance with what was reported previously (Hong et al. 2019, Zhao et al. 2020). The XRD results indicated that at two acidic and neutral pH the TC was adsorbed mainly on the interlayer spaces of all montmorillonite samples (the basal spacing was increased for 6 to 7 Å, Figure 5). However, at pH 9 for two samples that were not acid-treated no changes in the interlayer spaces was detected showing no adsorption of TC between interlayer spaces. while for the acid-treated (nanoporous montmorillonite samples) at pH of 9, a tween peak was detected showing a mutual adsorption of TC in the interlayer spaces and on the external surfaces of the samples (this trend is in accordance with the intraparticle diffusion models, Figure 4 and Table 3). The reason for adsorption of TC in the interlayer spaces of the nanoporous montmorillonite at pH 9 is the increase in the cation charges (H^+) in the interlayer spaces created during the acid treatment which allows TC to diffuse in the interlayer spaces and increase the basal spacing (TC is negatively charged at this pH) (Chahardahmasoumi et al. 2019). Enrichment of the montmorillonite with Fe ion did not change the trend of TC adsorption on the external surface or into the basal spacing of different samples (Figure 5).

Surprisingly, more than 30% of adsorbed TC was desorbed from all samples with a linear trend at all pH conditions (Figure 4), showing that the montmorillonite (natural or nanoporous one) could not fully immobilize TC in its structure and release it back to the environment in high amount. Higher amounts of TC were desorbed from the montmorillonite samples at pH of 9 (Figure 4) indicating more repulsion forces between the montmorillonite and the TC. The observed desorption of TC from montmorillonite samples was somehow expected as reported previously, however, compared to the desorption rate from agricultural soil (Conde-Cid et al. 2020), such a high amount of desorption was contrary to expectation (Figure 4). This phenomenon is partly due to the different nature of the adsorbents and partly due to the extremely low concentration of TC in the solution (in the range of 0.003 to 0.2 mg/ml) for adsorption onto the agricultural soil (Conde-Cid et al. 2019). However, by increasing the TC concentration in the solution the amount of TC adsorbed was increased (Figure 4) and the desorption rate onto the montmorillonite samples increased as well, which is a realistic prediction of the empirical situation. Hence, as the montmorillonite might reach its maximum adsorption capacity it finally releases the adsorbed TC to the environment. This could be a big challenge in the use of such environmentally friendly and cheap adsorbents for adsorption/separation of antibiotics such as TC. One possible remediation for such a problem is to apply a second capability on the montmorillonite to degrade the TC in the adsorption-desorption cycle. Hence the desorbed pollutants do not harm the environment upon desorption. A possible remediation process is to apply a photo-Fenton enhanced surface for photodegradation of TC. The Fe ions were loaded on the montmorillonite for this purpose and the properties of montmorillonite on the degradation of TC during the desorption process were analyzed.

To check the photocatalytic properties of montmorillonite samples, after adsorption of the TC, the montmorillonite was separated and put in a solution of the same pH and the light irradiation was applied

under shaking. Then the antibacterial activity test on the solution was done in different duration and the results were compared with the results of the antibacterial activity of the same sample in which the adsorption-desorption cycle were carried out in dark. Antibacterial activity results and the inhibition zone summary results of released TC from montmorillonite samples were plotted in Figures 6 and 7, respectively.

For the Mt and NP-Mt sample, almost no changes in the antimicrobial activity of the TC were detected after irradiation under light for up to 180 minutes at all pH compared to samples in dark (the inhibition zone in Figure $6a_1$, $6b_1$, $6c_1$, $6a_3$, $6b_3$, $6c_3$, and 7). By icreasing the desorption duration the inhibition zone increased (Figure 7) up to 120 minutes due to the increasing amount of TC desorbed and after that almost remained constant. Comparing the samples under light and in dark (comparing disk 1 with 4, 2 with 5, and 3 with 6 in Figure 6) the inhibition zone did not vary very much when placed under light for these two montmorillonite samples. Hence, the main conclusion is that the TC is desorbed from the montmorillonite and reasonably strong antimicrobial activity was detected even after being under light for 180 min. Considering the application of such adsorbent in the environment, montmorillonite does not perfectly separate the TC from the soil and release it back to the environment with almost no changes.

On the other hand, for the Fe saturated samples, the antibacterial activity of TC was reduced significantly even after 60 minutes of light irradiation (Figure $6a_2$, $6b_2$, $6c_2$, $6a_4$, $6b_4$, $6c_4$, and 7). The reduction in the antimicrobial activity of TC was higher for the nanoporous Fe saturated montmorillonite than the normal Fe saturated montmorillonite. The main reason could be the higher accessible site for the adsorption and possible photodegradation process. Indeed, the higher transparent nanoporous structure provides a higher chance for interlayer adsorbed TC to absorb light and be degraded. By increasing the light irradiation time from 60 to 180 the antimicrobial activity reduced steadily for Fe saturated samples compared to the same samples in dark. Therefore, during the desorption, the degradation of the TC occurs for Fe saturated samples and this process continues in an equilibrium adsorption-desorption-photodegradation cycle. Meanwhile, the degradation of TC was facilitated at acidic conditions due to the higher amount of TC desorbed from the montmorillonite samples (Figure 4) and a lower chance of degradation.

It is proposed that the photodegradation happens through a photo-Fenton process in which the Fe cations seemingly played a key role in the photo-Fenton deactivation of TC (Wang et al. 2020b). Fe cations degraded the TC by the production of active species via Fenton-type reaction. The production of $^{\cdot}OH$ radicals is the key element in the degradation of the TC via creating complexation (Brillas &Garcia-Segura 2020, Fareed et al. 2021, Liu et al. 2021b). Although the mechanism of the H_2O_2 decomposition in the photo-Fenton reaction is not well understood, the following reactions have been suggested corresponding the reduction of Fe^{3+} with the production of $^{\cdot}HO_2$ radicals, followed by regeneration of Fe^{3+} which resulted in the generation of the hydroxyl radicals (Ramirez et al. 2007):

$$X\text{-}Fe^{3+} + H_2O_2 \rightarrow X\text{-}Fe^{2+} + {}^{\cdot}HO_2 + H^+ \quad (1)$$

$X\text{-}Fe^{2+} + H_2O_2 \rightarrow X\text{-}Fe^{3+} + OH^- + {}^{\cdot}HO$ (2)

$TC + {}^{\cdot}OH \rightarrow$ degraded TC (3)

in which the X represents the surface of the montmorillonite surface. The concentration of ˙OH radicals was evaluated using the coumarin method in which the produced ˙OH radicals would react with the coumarin and produce 7-hydroxycoumarin that is highly fluorescent (Louit et al. 2005) and can be detected with a spectrophotometer (Figure 8). The proposed reactions take place on the montmorillonite surface when enriched with the Fe cations (Scheme 1). Based on the proposed mechanism, the Fe saturation of the non-porous montmorillonite mainly occurs on the external surfaces (Scheme 1). The TC adsorbed on the surfaces of the montmorillonite would be in a part of the Fenton reaction in which the created ˙OH radicals (Figure 7) helps to degrade TC. However, for the nanoporous montmorillonite, the nanopores (Scheme 1), giving rise to a protonated (H^+) amorphous hydrous silica, provide high accessible surface area for adsorption of Fe cations (Wei et al. 2017). In this structure, the absorption of light would be much higher than the non-porous montmorillonite. Hence a great opportunity for the production of ˙OH radicals was proved by the fluorescence spectra (Figure 8) and hence the photo-Fenton reactions would occur.

4. Conclusion

In this study, we proposed a modification method to convert montmorillonite into Fe saturated nanoporous layered structure with high affinity in adsorption and photo-Fenton degradation properties against tetracycline. Via an acid-treatment process, the surface area of the montmorillonite was increased four times and a nanoporous structure with pore sizes around 1.5 nm was created. The nanoporous Fe saturated montmorillonite showed a high affinity in the adsorption of TC. The antibacterial tests indicated that more than 30% of adsorbed TC was released from the normal montmorillonite with high antibacterial activity. Enrichment of the nanoporous montmorillonite with Fe ions increased its photocatalytic activity (photo-Fenton properties) and almost more than 90% of desorbed TC was degraded under visible light. The nanoporous structure of the montmorillonite provided a higher surface area for photodegradation of the TC compared to normal Fe-enriched montmorillonite by a higher amount of ˙OH radicals created in the nanoporous structure which helps the degradation of TC. The results of this study provided a novel environmentally friendly adsorbent with photocatalytic activity against TC which can be of interest to many scientists in this field.

Declarations

5.1. Ethics approval and consent to participate

In this manuscript, no studies are involving human participants, human data, or human tissue.

5.2. Consent for publication

This manuscript does not contain any individual person's data in any form.

5.3. Availability of data and materials

The datasets used and/or analyzed during the current study are available from the corresponding author on reasonable request

5.4. Competing interests

The authors declare that they have no known competing financial interests or personal relationships that could have appeared to influence the work reported in this manuscript.

5.5. Funding

There is no funding available for this manuscript.

5.6. Authors' contributions

ShCh: Conceptualization, Methodology, Writing- Original draft preparation

SAHJ: Investigation, Supervision, Visualization

MNS: Validation, Methodology, Reviewing and Editing, Project administration

5.7. Acknowledgments

The authors are grateful for access to the infrastructure provided by the Department of Mining Engineering of the Isfahan University of Technology.

References

1. Ahsan MA, Katla SK, Islam MT, Hernandez-Viezcas JA, Martinez LM, Díaz-Moreno CA, Lopez J, Singamaneni SR, Banuelos J, Gardea-Torresdey J, Noveron JC (2018) Adsorptive removal of methylene blue, tetracycline and Cr(VI) from water using sulfonated tea waste. Environmental Technology Innovation 11:23–40
2. Akbari Alavijeh M, Sarvi MN, Ramazani Afarani Z (2017) Properties of adsorption of vitamin B12 on nanoclay as a versatile carrier. Food Chem 219:207–214
3. Ambrogi V, Latterini L, Nocchetti M, Pagano C, Ricci M (2012) Montmorillonite as an agent for drug photostability. J Mater Chem 22:22743–22749
4. Ambrogi V, Nocchetti M, Latterini L (2014) Promethazine–Montmorillonite Inclusion Complex To Enhance Drug Photostability. Langmuir 30:14612–14620
5. Ameta R, Chohadia K, Jain A, Punjabi A PB (2018) Chapter 3 - Fenton and Photo-Fenton Processes. In: Ameta SC, Ameta R (eds) Advanced Oxidation Processes for Waste Water Treatment. Academic

Press, pp 49–87

6. Bieseki L, Treichel H, Araujo AS, Pergher SBC (2013) Porous materials obtained by acid treatment processing followed by pillaring of montmorillonite clays. Appl Clay Sci 85:46–52
7. Brillas E, Garcia-Segura S (2020) Benchmarking recent advances and innovative technology approaches of Fenton, photo-Fenton, electro-Fenton, and related processes: A review on the relevance of phenol as model molecule. Sep Purif Technol 237:116337
8. Bugueño-Carrasco S, Monteil H, Toledo-Neira C, Sandoval M, Thiam A, Salazar R (2021) Elimination of pharmaceutical pollutants by solar photoelectro-Fenton process in a pilot plant. Environ Sci Pollut Res 28:23753–23766
9. Carretero MI, Gomes CSF, Tateo F (2013) Chapter 5.5 - Clays, Drugs, and Human Health. In: Bergaya F, Lagaly G (eds) Developments in Clay Science. Elsevier, pp 711–764
10. Chahardahmasoumi S, Sarvi MN, Jalali SAH (2019) Modified montmorillonite nanosheets as a nanocarrier with smart pH-responsive control on the antimicrobial activity of tetracycline upon release. Appl Clay Sci 178:105135
11. Chen Q, Wu P, Li Y, Zhu N, Dang Z (2009) Heterogeneous photo-Fenton photodegradation of reactive brilliant orange X-GN over iron-pillared montmorillonite under visible irradiation. J Hazard Mater 168:901–908
12. Conde-Cid M, Fernández-Calviño D, Nóvoa-Muñoz JC, Núñez-Delgado A, Fernández-Sanjurjo MJ, Arias-Estévez M, Álvarez-Rodríguez E (2019) Experimental data and model prediction of tetracycline adsorption and desorption in agricultural soils. Environ Res 177:108607
13. Conde-Cid M, Ferreira-Coelho G, Arias-Estévez M, Fernández-Calvinho D, Núñez-Delgado A, Álvarez-Rodríguez E, Fernández-Sanjurjo MJ (2020) Adsorption/desorption of three tetracycline antibiotics on different soils in binary competitive systems. J Environ Manage 262:110337
14. Czili H, Horváth A (2008) Applicability of coumarin for detecting and measuring hydroxyl radicals generated by photoexcitation of TiO2 nanoparticles. Appl Catal B 81:295–302
15. Fareed A, Hussain A, Nawaz M, Imran M, Ali Z, Haq SU (2021) The impact of prolonged use and oxidative degradation of Atrazine by Fenton and photo-Fenton processes. Environmental Technology Innovation 24:101840
16. Figueroa RA, Leonard A, MacKay AA (2004) Modeling Tetracycline Antibiotic Sorption to Clays. Environmental Science Technology 38:476–483
17. Franco F, Pozo M, Cecilia JA, Benítez-Guerrero M, Lorente M (2016) Effectiveness of microwave assisted acid treatment on dioctahedral and trioctahedral smectites. The influence of octahedral composition. Appl Clay Sci 120:70–80
18. Gironi LC, Damiani G, Zavattaro E, Pacifico A, Santus P, Pigatto PDM, Cremona O, Savoia P (2021) Tetracyclines in COVID-19 patients quarantined at home: Literature evidence supporting real-world data from a multicenter observational study targeting inflammatory and infectious dermatoses. Dermatol Ther 34:e14694

19. Han C-H, Park H-D, Kim S-B, Yargeau V, Choi J-W, Lee S-H, Park J-A (2020) Oxidation of tetracycline and oxytetracycline for the photo-Fenton process: Their transformation products and toxicity assessment. Water Res 172:115514
20. Hassan AK, Rahman MM, Chattopadhay G, Naidu R (2019) Kinetic of the degradation of sulfanilic acid azochromotrop (SPADNS) by Fenton process coupled with ultrasonic irradiation or L-cysteine acceleration. Environmental Technology Innovation 15:100380
21. Hong R, Zhang L, Zhu W, Gu C (2019) Photo-transformation of atrazine in aqueous solution in the presence of Fe3+-montmorillonite clay and humic substances. Science of The Total Environment 652:224–233
22. Huang S, Zhang Q, Liu P, Ma S, Xie B, Yang K, Zhao Y (2020) Novel up-conversion carbon quantum dots/α-FeOOH nanohybrids eliminate tetracycline and its related drug resistance in visible-light responsive Fenton system. Appl Catal B 263:118336
23. Imanipoor J, Mohammadi M, Dinari M (2021) Evaluating the performance of L-methionine modified montmorillonite K10 and 3-aminopropyltriethoxysilane functionalized magnesium phyllosilicate organoclays for adsorptive removal of azithromycin from water. Sep Purif Technol 275:119256
24. Jain M, Mudhoo A, Ramasamy DL, Najafi M, Usman M, Zhu R, Kumar G, Shobana S, Garg VK, Sillanpää M (2020) Adsorption, degradation, and mineralization of emerging pollutants (pharmaceuticals and agrochemicals) by nanostructures: a comprehensive review. Environ Sci Pollut Res 27:34862–34905
25. Jayrajsinh S, Shankar G, Agrawal YK, Bakre L (2017) Montmorillonite nanoclay as a multifaceted drug-delivery carrier: A review. Journal of Drug Delivery Science Technology 39:200–209
26. Jiao S, Zheng S, Yin D, Wang L, Chen L (2008) Aqueous photolysis of tetracycline and toxicity of photolytic products to luminescent bacteria. Chemosphere 73:377–382
27. Li Z, Ma H, Zang L, Li D, Guo S, Shi L (2021) Construction of nano-flower MIL-125(Mo)-In2Se3 Z-scheme heterojunctions by one-step solvothermal method for removal of tetracycline from wastewater in the synergy of adsorption and photocatalysis way. Sep Purif Technol 276:119355
28. Liu Y, Chen Y, Feng M, Chen J, Shen W, Zhang S (2021a) Occurrence of antibiotics and antibiotic resistance genes and their correlations in river-type drinking water source, China. Environ Sci Pollut Res 28:42339–42352
29. Liu Y, Zhao Y, Wang J (2021b) Fenton/Fenton-like processes with in-situ production of hydrogen peroxide/hydroxyl radical for degradation of emerging contaminants: Advances and prospects. J Hazard Mater 404:124191
30. Louit G, Foley S, Cabillic J, Coffigny H, Taran F, Valleix A, Renault JP, Pin S (2005) The reaction of coumarin with the OH radical revisited: hydroxylation product analysis determined by fluorescence and chromatography. Radiat Phys Chem 72:119–124
31. Lu Z, He F, Hsieh CY, Wu X, Song M, Liu X, Liu Y, Yuan S, Dong H, Han S, Du P, Xing G (2019a) Magnetic Hierarchical Photocatalytic Nanoreactors: Toward Highly Selective Cd2+ Removal with Secondary Pollution Free Tetracycline Degradation. ACS Applied Nano Materials 2:1664–1674

32. Lu Z, Peng J, Song M, Liu Y, Liu X, Huo P, Dong H, Yuan S, Ma Z, Han S (2019b) Improved recyclability and selectivity of environment-friendly MFA-based heterojunction imprinted photocatalyst for secondary pollution free tetracycline orientation degradation. Chem Eng J 360:1262–1276
33. Madejová J (2003) FTIR techniques in clay mineral studies. Vib Spectrosc 31:1–10
34. Maezono T, Tokumura M, Sekine M, Kawase Y (2011) Hydroxyl radical concentration profile in photo-Fenton oxidation process: Generation and consumption of hydroxyl radicals during the discoloration of azo-dye Orange II. Chemosphere 82:1422–1430
35. Maged A, Kharbish S, Ismael IS, Bhatnagar A (2020) Characterization of activated bentonite clay mineral and the mechanisms underlying its sorption for ciprofloxacin from aqueous solution. Environ Sci Pollut Res 27:32980–32997
36. Maroga Mboula V, Héquet V, Gru Y, Colin R, Andrès Y (2012) Assessment of the efficiency of photocatalysis on tetracycline biodegradation. J Hazard Mater 209-210:355–364
37. Mosaleheh N, Sarvi MN (2020) Minimizing the residual antimicrobial activity of tetracycline after adsorption into the montmorillonite: Effect of organic modification. Environ Res 182:109056
38. Mosquera-Sulbaran JA, Hernández-Fonseca H (2021) Tetracycline and viruses: a possible treatment for COVID-19? Arch Virol 166:1–7
39. Niu L, Zhang G, Xian G, Ren Z, Wei T, Li Q, Zhang Y, Zou Z (2021) Tetracycline degradation by persulfate activated with magnetic γ-Fe2O3/CeO2 catalyst: Performance, activation mechanism and degradation pathway. Sep Purif Technol 259:118156
40. Norvill ZN, Toledo-Cervantes A, Blanco S, Shilton A, Guieysse B, Muñoz R (2017) Photodegradation and sorption govern tetracycline removal during wastewater treatment in algal ponds. Biores Technol 232:35–43
41. Ramazani Afarani Z, Sarvi MN, Akbari Alavijeh M (2018) Modification of montmorillonite nanolayers as a pH-responsive carrier of biomolecules: Delivery of vitamin B12. J Taiwan Inst Chem Eng 84:19–27
42. Ramirez JH, Costa CA, Madeira LM, Mata G, Vicente MA, Rojas-Cervantes ML, López-Peinado AJ, Martín-Aranda RM (2007) Fenton-like oxidation of Orange II solutions using heterogeneous catalysts based on saponite clay. Appl Catal B 71:44–56
43. Shen Q, Wang Z, Yu Q, Cheng Y, Liu Z, Zhang T, Zhou S (2020) Removal of tetracycline from an aqueous solution using manganese dioxide modified biochar derived from Chinese herbal medicine residues. Environ Res 183:109195
44. Sing KSW (1985) Reporting physisorption data for gas/solid systems with special reference to the determination of surface area and porosity (Recommendations 1984). Pure Appl Chem 57:603–619
45. Temuujin J, Jadambaa T, Burmaa G, Erdenechimeg S, Amarsanaa J, MacKenzie KJD (2004) Characterisation of acid activated montmorillonite clay from Tuulant (Mongolia). Ceram Int 30:251–255

46. Thomas N, Dionysiou DD, Pillai SC (2021) Heterogeneous Fenton catalysts: A review of recent advances. J Hazard Mater 404:124082
47. Tong C, Jing L, He M, Xie M, Wei W, Xu Y, Xu H, Li H (2021) Construction of dual ion (Fe3+/Fe2+ and Nb5+/Nb4+) synergy and full spectrum 1D nanorod Fe2O3/NaNbO3 photo-Fenton catalyst for the degradation of antibiotic: Effects of H2O2, S2O82– and toxicity. Sep Purif Technol 261:118269
48. Starling VM, Costa MC, Souza EP, Machado FA, de Araujo EC, Amorim JC CC (2021) Persulfate mediated solar photo-Fenton aiming at wastewater treatment plant effluent improvement at neutral PH: emerging contaminant removal, disinfection, and elimination of antibiotic-resistant bacteria. Environ Sci Pollut Res 28:17355–17368
49. Veiskarami M, Sarvi MN, Mokhtari AR (2016) Influence of the purity of montmorillonite on its surface modification with an alkyl-ammonium salt. Appl Clay Sci 120:111–120
50. Verma M, Haritash AK (2020) Photocatalytic degradation of Amoxicillin in pharmaceutical wastewater: A potential tool to manage residual antibiotics. Environmental Technology Innovation 20:101072
51. Wang A, Zheng Z, Wang H, Chen Y, Luo C, Liang D, Hu B, Qiu R, Yan K (2020a) 3D hierarchical H2-reduced Mn-doped CeO2 microflowers assembled from nanotubes as a high-performance Fenton-like photocatalyst for tetracycline antibiotics degradation. Appl Catal B 277:119171
52. Wang X, Zhang X, Zhang Y, Wang Y, Sun S-P, Wu WD, Wu Z (2020b) Nanostructured semiconductor supported iron catalysts for heterogeneous photo-Fenton oxidation: a review. Journal of Materials Chemistry A 8:15513–15546
53. Wang Z, Muhammad Y, Tang R, Lu C, Yu S, Song R, Tong Z, Han B, Zhang H (2021) Dually organic modified bentonite with enhanced adsorption and desorption of tetracycline and ciprofloxacine. Sep Purif Technol 274:119059
54. Wei X, Wu H, He G, Guan Y (2017) Efficient degradation of phenol using iron-montmorillonite as a Fenton catalyst: Importance of visible light irradiation and intermediates. J Hazard Mater 321:408–416
55. Wu Q, Que Z, Li Z, Chen S, Zhang W, Yin K, Hong H (2018) Photodegradation of ciprofloxacin adsorbed in the intracrystalline space of montmorillonite. J Hazard Mater 359:414–420
56. Yuan P, Annabi-Bergaya F, Tao Q, Fan M, Liu Z, Zhu J, He H, Chen T (2008) A combined study by XRD, FTIR, TG and HRTEM on the structure of delaminated Fe-intercalated/pillared clay. J Colloid Interface Sci 324:142–149
57. Zhang Y, Jiao Z, Hu Y, Lv S, Fan H, Zeng Y, Hu J, Wang M (2017) Removal of tetracycline and oxytetracycline from water by magnetic Fe3O4@graphene. Environ Sci Pollut Res 24:2987–2995
58. Zhao Y, Gu X, Li S, Han R, Wang G (2015) Insights into tetracycline adsorption onto kaolinite and montmorillonite: experiments and modeling. Environ Sci Pollut Res 22:17031–17040
59. Zhao Y, Kang S, Qin L, Wang W, Zhang T, Song S, Komarneni S (2020) Self-assembled gels of Fe-chitosan/montmorillonite nanosheets: Dye degradation by the synergistic effect of adsorption and photo-Fenton reaction. Chem Eng J 379:122322

Scheme

Scheme 1 is available in the Supplemental Files section.

Figures

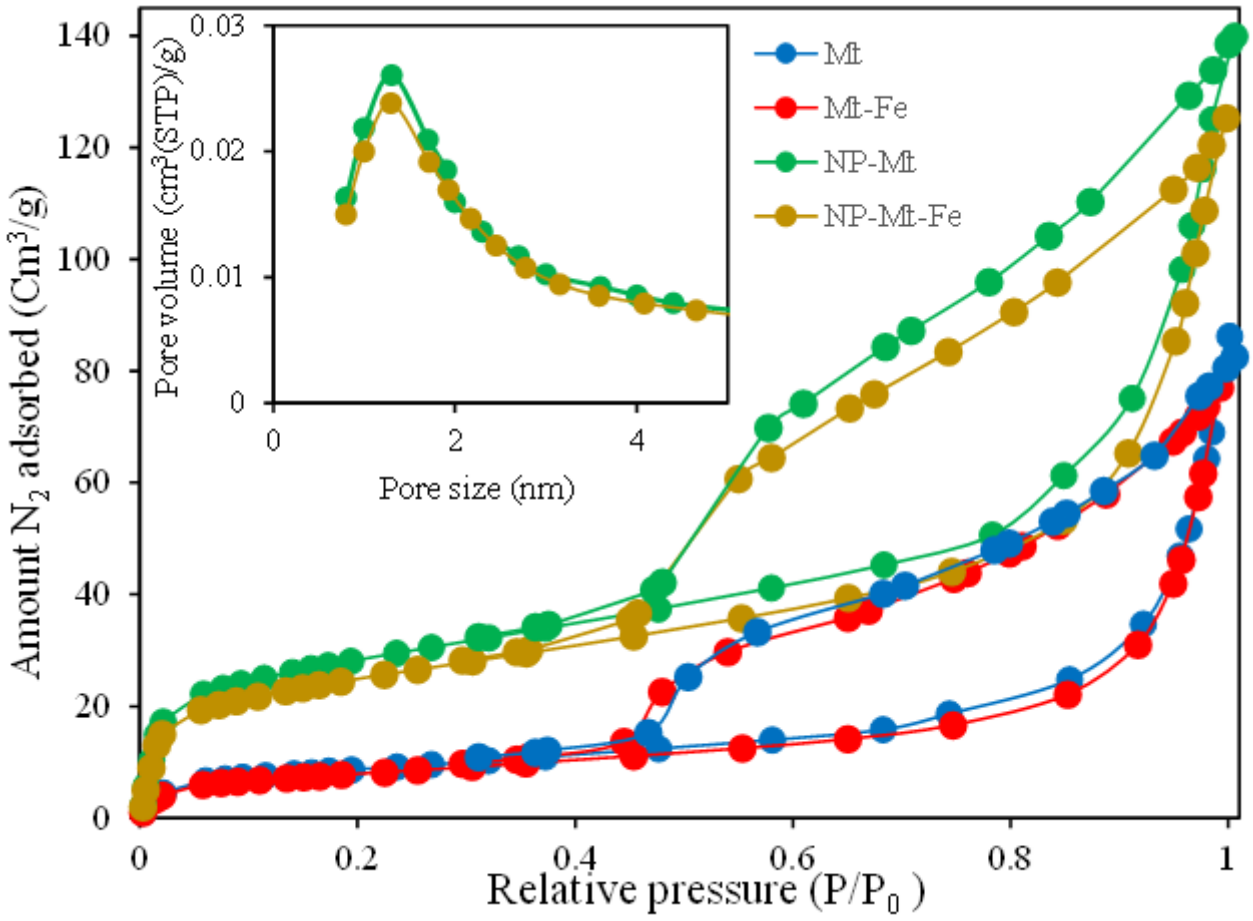

Figure 1

Nitrogen sorption isotherms of different samples.

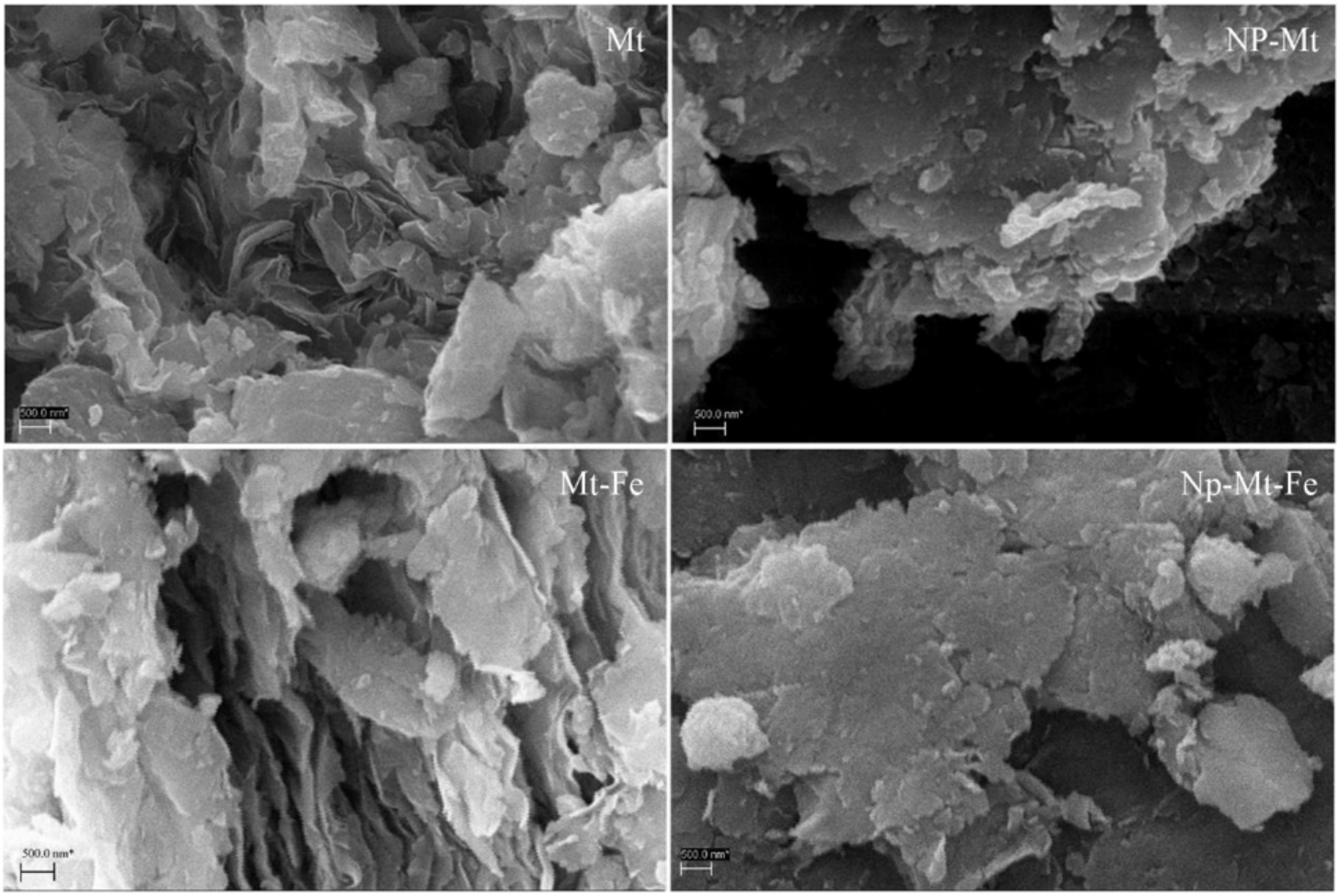

Figure 2

SEM images of montmorillonite samples (scale bars are 500 nm in all images).

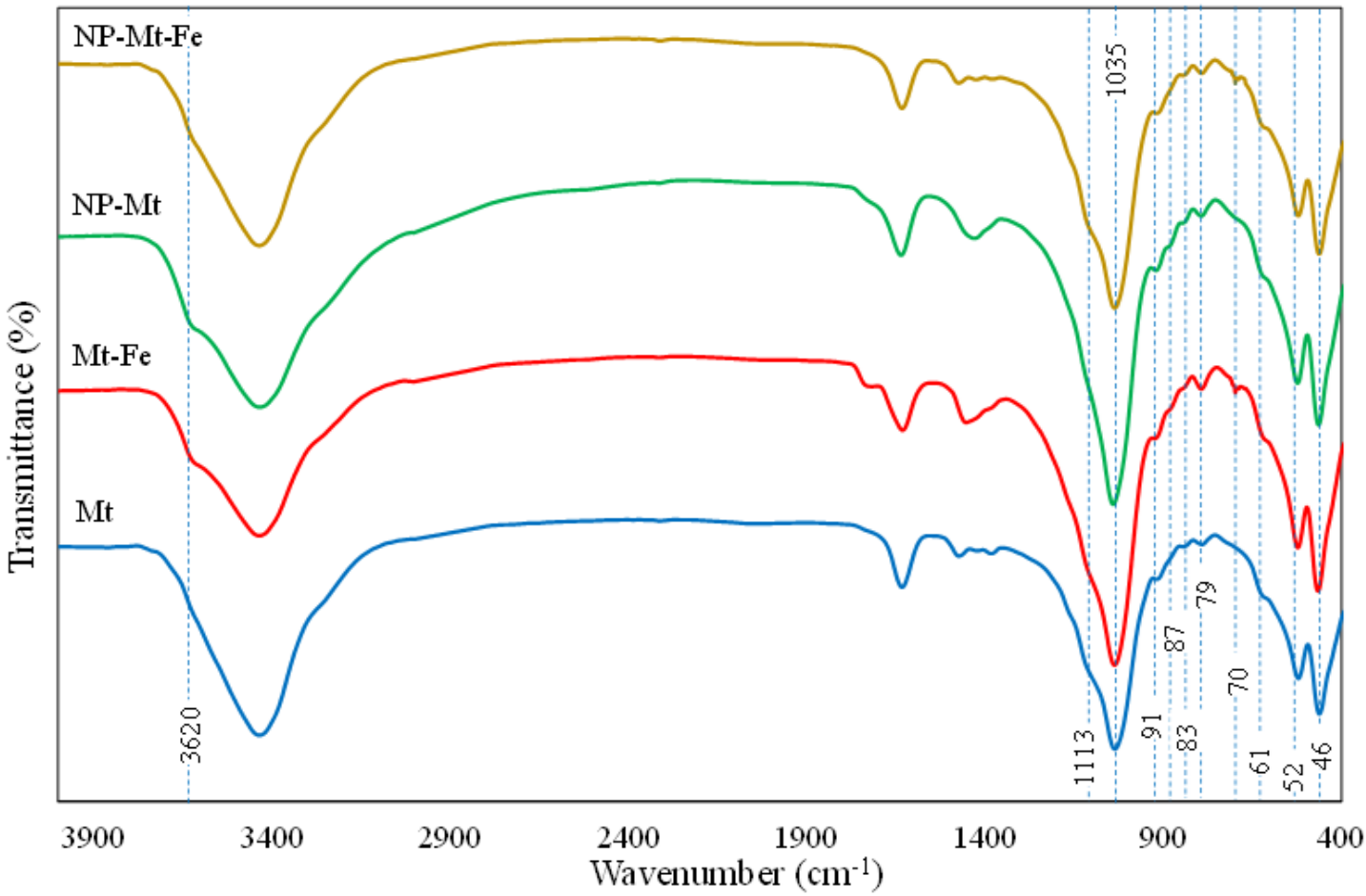

Figure 3

FTIR analysis of montmorillonite samples

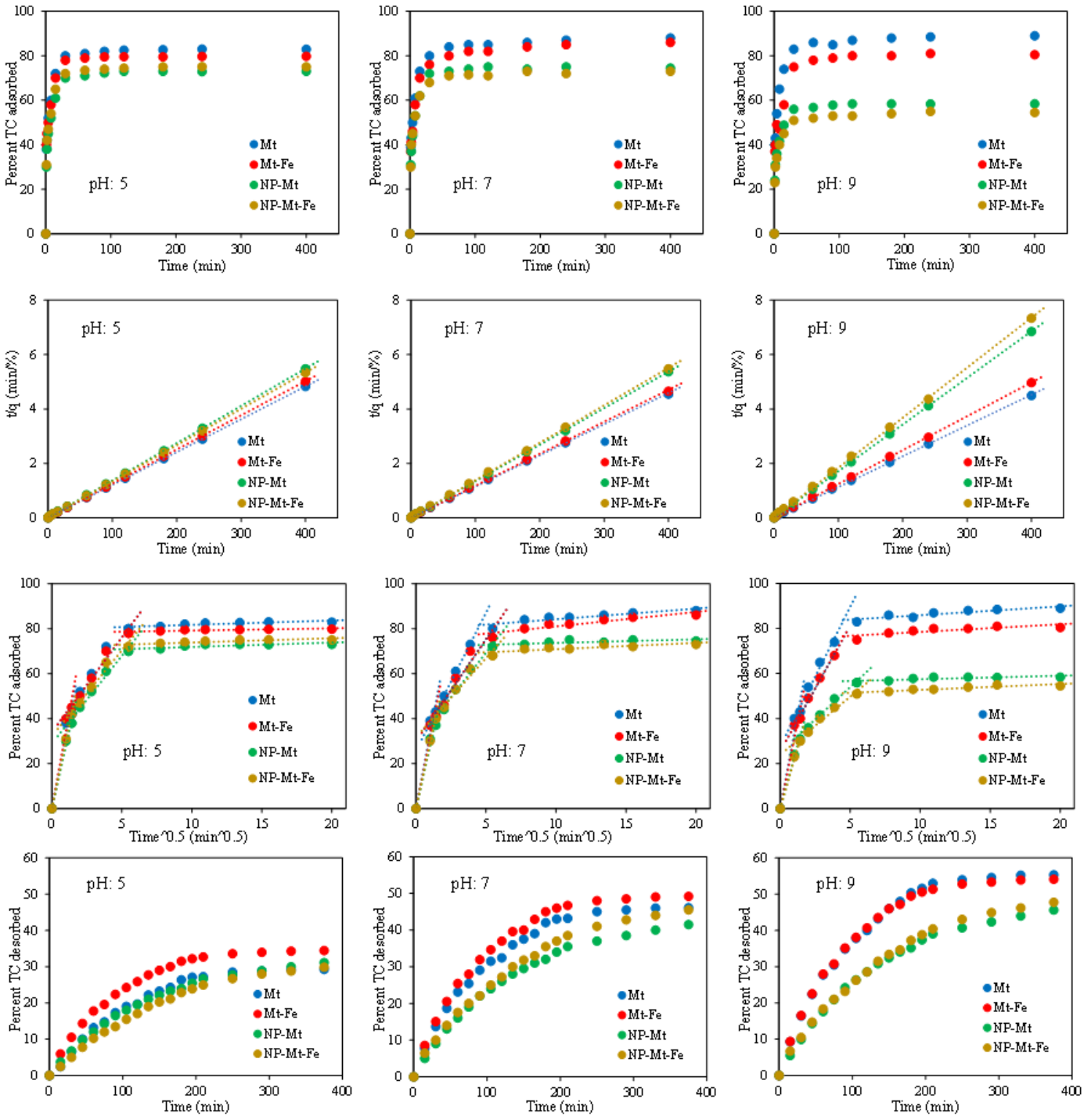

Figure 4

Kinetics of absorption, kinetics models fitted to the adsorption results (pseudo-second-order and intraparticle diffusion), and kinetics of desorption of the TC from different montmorillonite samples.

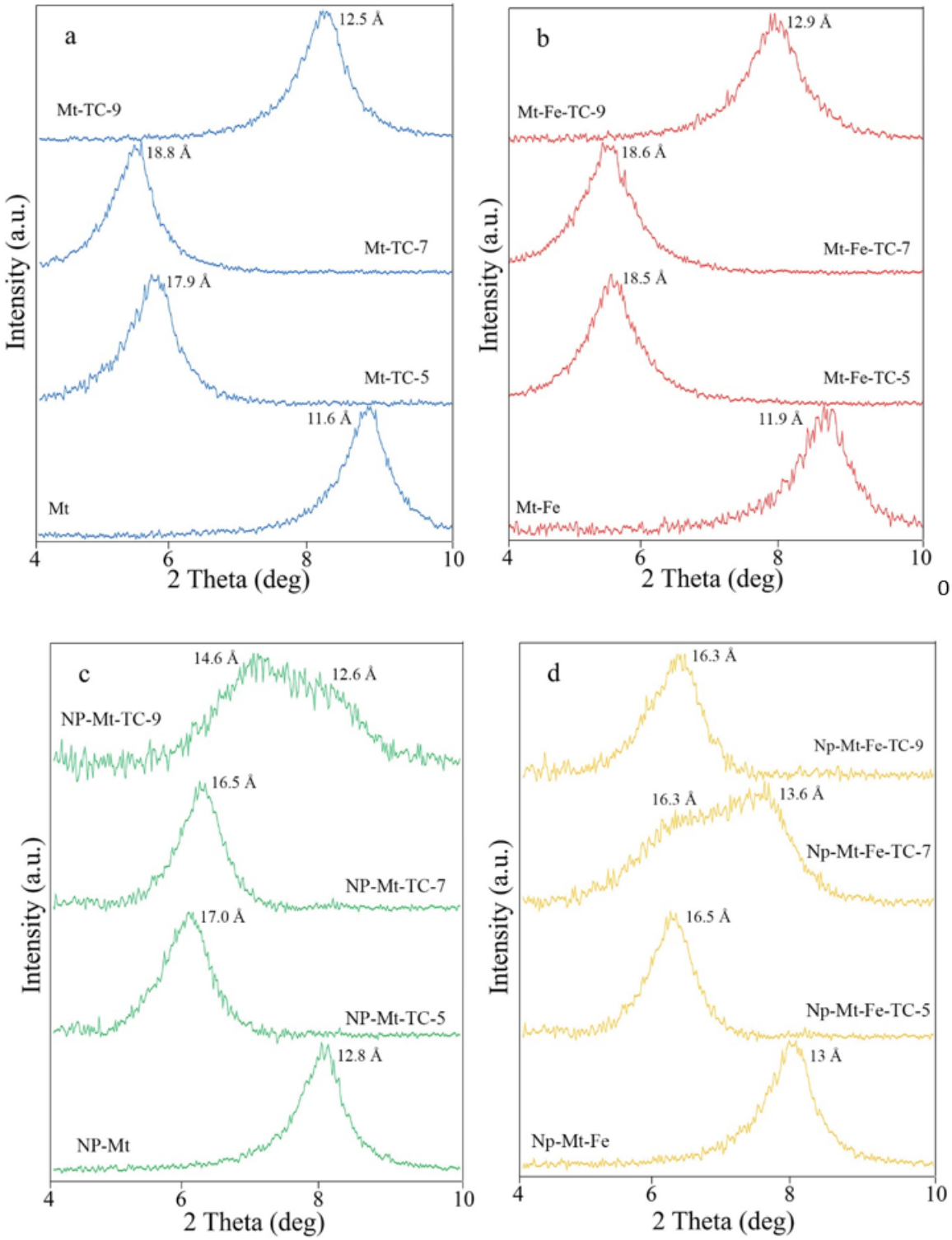

Figure 5

The XRD results of different montmorillonites samples before and after adsorption of TC.

Figure 6

Antibacterial activity results of desorbed TC against Escherichia coli after light irradiation for different samples (index 1, 2, 3, and 4 represent samples Mt, Mt-Fe, NP-Mt, and NP-Mt-Fe, respectively) at different light irradiation (disk 1, 2 and 3 being under light for 60, 120, and 180 minues, respectively; and distks 4, 5, and 6 corresponding same sample of 1, 2, and 3 which was in dark), at different pH (a, b, and c represent pH of 5, 7, and 9, respectively).

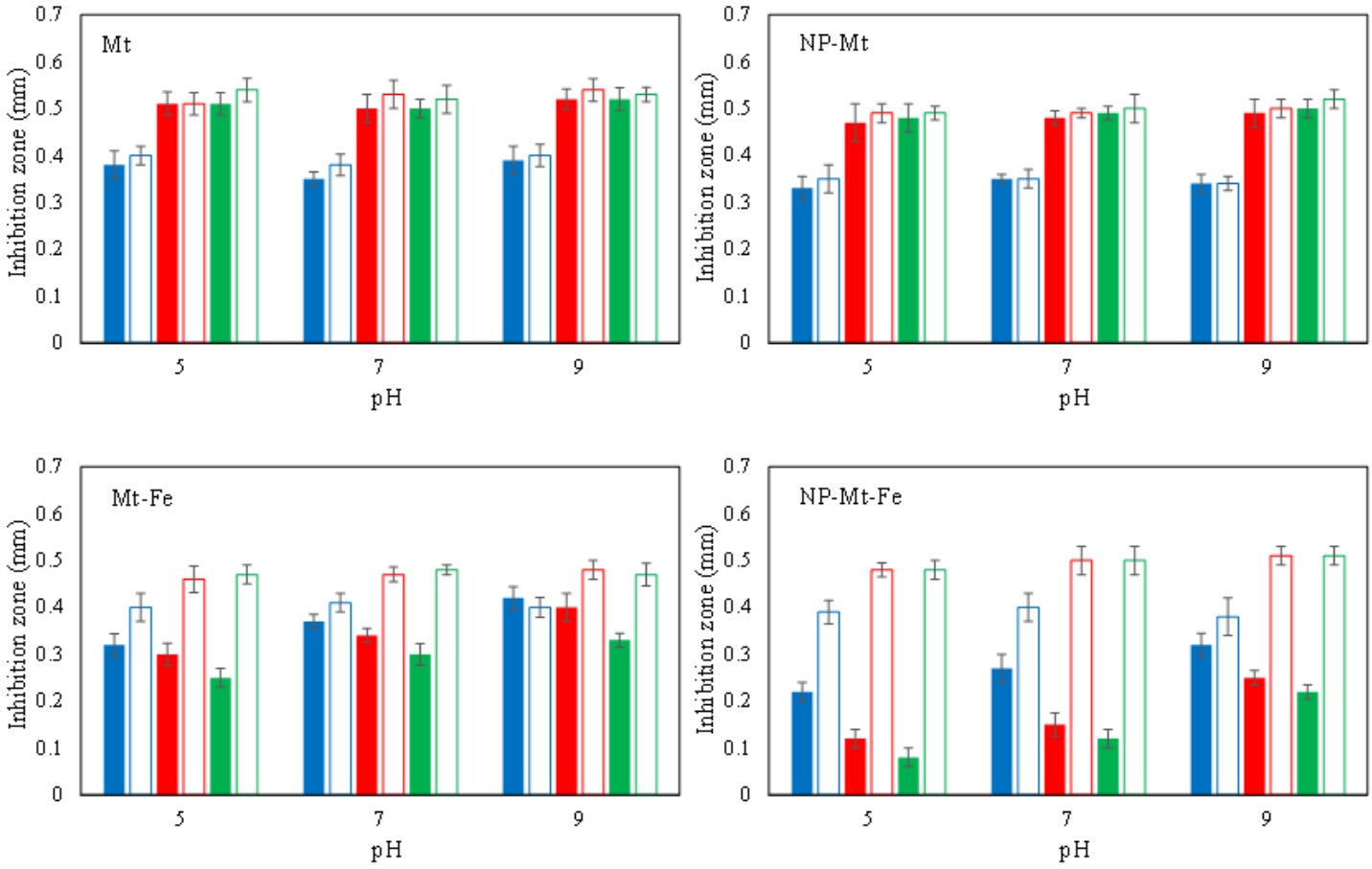

Figure 7

Details of inhibition zone (annular radius) indicating the antimicrobial activity of TC after photodegradation test for the different duration (solid filled bar charts, 60 min: blue, 120 min: red, and 180 min: green) along with the control samples in dark (not-filled bar charts)

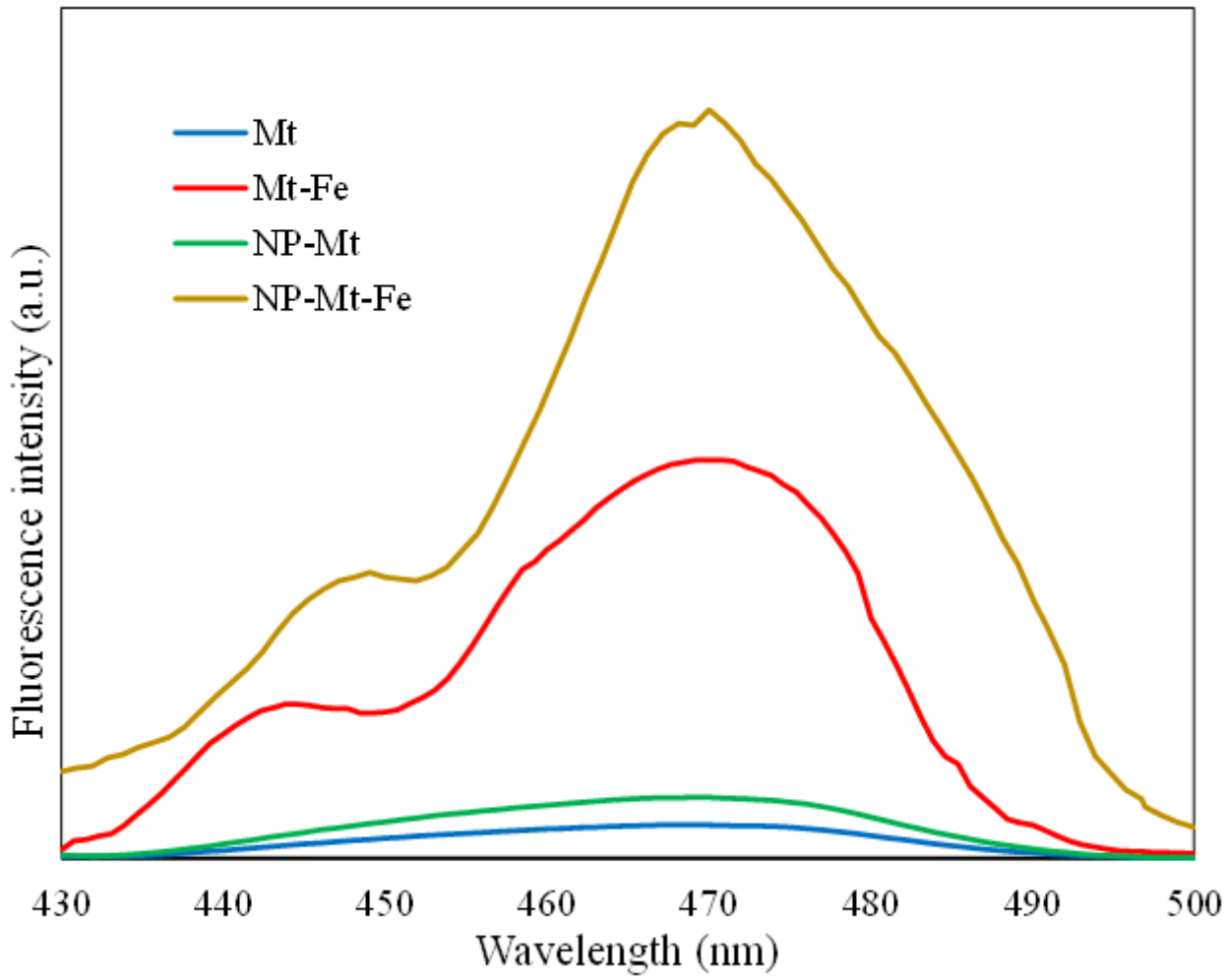

Figure 8

Fluorescence spectra of the sample taken from the solution containing different montmorillonite samples after being under irradiation under UV for 5 minutes

Supplementary Files

This is a list of supplementary files associated with this preprint. Click to download.

- Scheme1.png